Available online at www.sciencedirect.com
ScienceDirect
Journal of Power Sources 160 (2006) 1506–1510
JOURNAL OF POWER SOURCES
www.elsevier.com/locate/jpowsour

Short communication

Effect of temperature annealing on capacitive and structural properties of hydrous ruthenium oxides

Wei-Chuan Fang [a], Jin-Hua Huang [a,*], Li-Chyong Chen [b], Yuh-Long Oliver Su [c], Kuei-Hsien Chen [d]

[a] *Department of Materials Science and Engineering, National Tsing Hua University, Hsinchu 300, Taiwan*
[b] *Center for Condensed Matter Sciences, National Taiwan University, Taipei, Taiwan*
[c] *Department of Applied Chemistry, National Chi Nan University, Puli 545, Nantou, Taiwan*
[d] *Institute of Atomic and Molecular Sciences, Academia Sinica, Taipei, Taiwan*

Received 14 January 2006; received in revised form 7 March 2006; accepted 9 March 2006
Available online 27 April 2006

Abstract

The structure–property relationships of hydrous ruthenium oxides, fabricated by electro deposition on Ti foil, were investigated with different annealing conditions. The annealing temperature was found to play an important role in affecting the electrochemical performance of the annealed hydrous ruthenium oxides. The results indicate that annealing hydrous ruthenium oxide at its crystallization threshold temperature, ∼200 °C, may help to create suitable nanostructure in the oxide that supports the establishment of interpenetrating percolation paths for balanced electron and proton conduction, thereby improving the capacitive response of the oxide dramatically. This finding is useful for fabrication of electrodes with enhanced electrochemical performance for application in microsupercapacitor.

Keywords: Supercapacitor; Hydrous ruthenium oxides; Annealing effect

1. Introduction

Supercapacitors [1] are energy storage devices, which have attracted considerable interest over the past decade. Presently, they have been applied to MEMS, microrobots, and implantable medical devices [2,3]. This is because in micropower devices application, the thin-film battery is insufficient to provide adequate power density required for ignition, and therefore unable to sustain an acceptable working power for a long period of time. Microsupercapacitor with enhanced pulse current and extended lifetime would be the most promising alternative.

Ruthenium oxide has been used as electrode material for supercapacitors because of its enormous capacitive behavior [4–6]. This type of capacitor is usually constructed in the form of bulk and its pseudo-capacitive property is attributed to the hydrogen ion induced electrochemical reaction. Therefore, hydrogen ions diffusion problem in the inner bulk of the oxide at high scan rates has resulted in the decayed capacitive performance [5]. Ruthenium oxide is usually hydrous and conduction mechanisms in the oxide involve both the electron and proton conductivities [7]. The electron conductivity improves with crystallinity of the oxide. On the contrary, the proton conductivity dominates when the crystallinity of the oxide degraded. So far, studies related to this issue have not been investigated in detail. In this work, the effects of annealing treatment on the structural and electrochemical properties of ruthenium oxide were investigated. This study may offer a practical way to improve the electrochemical behavior of ruthenium oxide with better capacitive performance for application in microsupercapacitor.

2. Experimental

Hydrous ruthenium oxide thin films ($RuO_2{\cdot}xH_2O$) were electrodeposited on polished Ti foils from an aqueous solution containing 0.05 M $RuCl_3$, 0.01 M HCl, and 0.1 M KCl. The depositions were carried out in a potential window of −1 to 1 V for 30 scan cycles at 20 mV s^{-1}. Good adhesion was achieved by

* Corresponding author. Tel.: +886 3 5162228; fax: +886 3 5722366.
E-mail address: jihhuang@mx.nthu.edu.tw (J.-H. Huang).

0378-7753/$ – see front matter © 2006 Elsevier B.V. All rights reserved.
doi:10.1016/j.jpowsour.2006.03.017

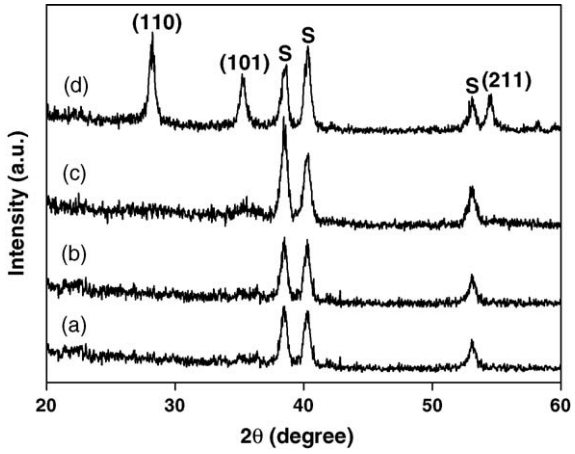

Fig. 1. XRD patterns of $RuO_2{\cdot}xH_2O$ either (a) as-prepared, or annealed in air for 2 h at (b) 100 °C, (c) 200 °C, and (d) 400 °C.

keeping the deposition bath temperature at 50 °C. After deposition, the films were annealed in air at 100, 200, and 400 °C for 2 h. The morphologies and structures of ruthenium oxides were analyzed with scanning electron microscopy (SEM), X-ray diffraction (XRD), X-ray photoelectron spectroscopy (XPS), and Raman spectroscopy. Electrochemical analysis and electrodeposition were carried out in a μAutolab Potentiostat/Galvanostat Type III station. An aqueous solution of 1 M H_2SO_4 was used as the electrolyte. Cyclic voltammetry responses were acquired after 10 cycles at a scan rate of 20 mV s^{-1}.

3. Results and discussion

Information on the crystalline nature of the annealed $RuO_2{\cdot}xH_2O$ obtained from XRD is shown in Fig. 1. The diffractions of the oxides annealed in air at temperatures $\leq$100 °C show characteristic peaks associated with the Ti foil located at 37°, 40° and 53°. The absence of diffraction peaks corresponding to RuO_2 implies that the $RuO_2{\cdot}xH_2O$ is amorphous. After 200 °C annealing treatment, a diffuse scattering peak appeared at 36°, suggesting the instigation of an amorphous to crystalline phase transformation. When the annealing temperature is raised to 400 °C, three sharp peaks located at 28°, 36°, and 54° corresponding to anhydrous RuO_2 (1 1 0), (1 0 1) and (2 1 1) orientations are clearly observed, indicating long-range crystalline order.

The SEM morphologies of pristine and annealed $RuO_2{\cdot}xH_2O$ are shown in Fig. 2. In Fig. 2(a), the pristine $RuO_2{\cdot}xH_2O$ possesses non-uniformly distributed aggregates giving rise to a high surface roughness. After 100 °C annealing treatment, the degree of uniformity is enhanced, implying that heat treatment promotes the surface diffusion of the constituents. After 200 °C

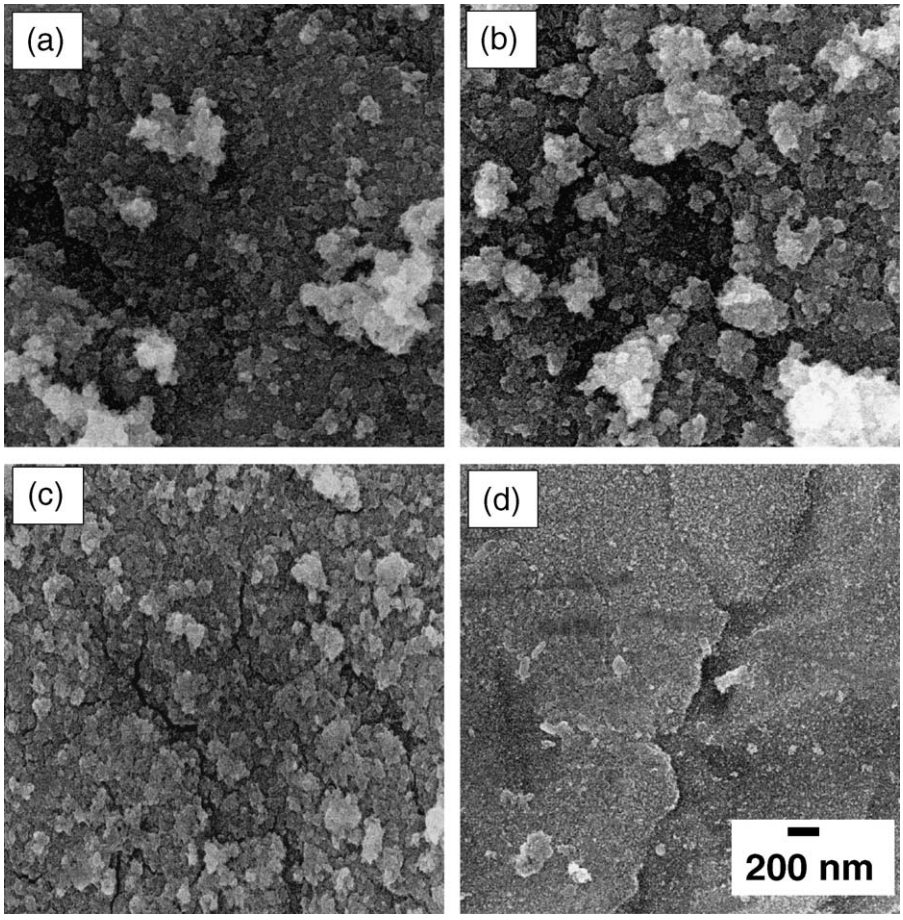

Fig. 2. SEM images of $RuO_2{\cdot}xH_2O$ either (a) as-prepared, or annealed in air for 2 h at (b) 100 °C, (c) 200 °C, and (d) 400 °C.

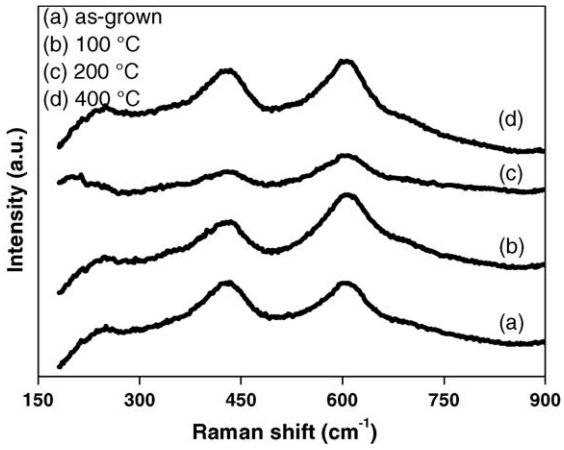

Fig. 3. Raman spectra of $RuO_2{\cdot}xH_2O$ either (a) as-prepared, or annealed in air for 2 h at (b) 100 °C, (c) 200 °C, and (d) 400 °C.

annealing treatment, the morphology of the oxide exhibits some cracking suggesting the occurrence of a dehydration process. When the annealing temperature is raised to 400 °C, the oxide surface is smooth with uniform distribution.

Fig. 3 presents the Raman spectra of $RuO_2{\cdot}xH_2O$ annealed at various temperatures. The films exhibit distinct vibrational peaks located at 240, 435, and 615 cm^{-1} even though the three major Raman bands, namely E_g, A_{1g}, and B_{2g} modes of RuO_2 were found to locate at ~528, 646, and 716 cm^{-1}, respectively [8]. It has been well known that vibrational frequencies of Raman spectrum can be significantly influenced by physical and/or chemical processes [9]. Although the observed peak positions are significantly different from those of RuO_2 characteristic bands, they consistently appeared under different temperature treatments. It implies that $RuO_2{\cdot}xH_2O$ has been successfully deposited on Ti foils. The most striking change in the Raman spectra is the shifting of the band at 240 cm^{-1} towards a lower wavenumber at annealing temperature of 200 °C.

Typical XPS core level spectra of O 1s and Ru 3p for pristine and annealed $RuO_2{\cdot}xH_2O$ are shown in Fig. 4. The O 1s core level peak is located at 536 eV for pristine and 100 °C-annealed hydrous RuO_2. However, the O 1s peak position shifts down to 529 eV and shifts up to 534 eV after 200 and 400 °C annealing treatments, respectively. The Ru 3p core level peak is located at 490 eV for pristine and 100 °C-annealed hydrous RuO_2. Likewise, the Ru 3p peak position shifts to a lower energy of 484 eV at 200 °C and shifts to a higher energy of 488 eV at 400 °C. This result demonstrates the occurrence of phase transformations in $RuO_2{\cdot}xH_2O$ as the molecular water component is decreased. The shift of the Ru 3p and O 1s peaks towards lower energy at 200 °C is consistent with the work of Chang and Hu [10]. According to [10], the energy spectrum of O 1s is positioned between 525 and 537 eV and that of Ru 3p is between 456 and 472 eV. In the present work, the energy spectrum of O 1s is placed between 533 and 539 eV and that of Ru 3p between 486 and 493 eV. Obviously, the positioning of the energy levels in the present work is towards higher binding energies and the similar shifting phenomenon is also encountered in the Raman spectra. It is probably related to the intrinsic difference

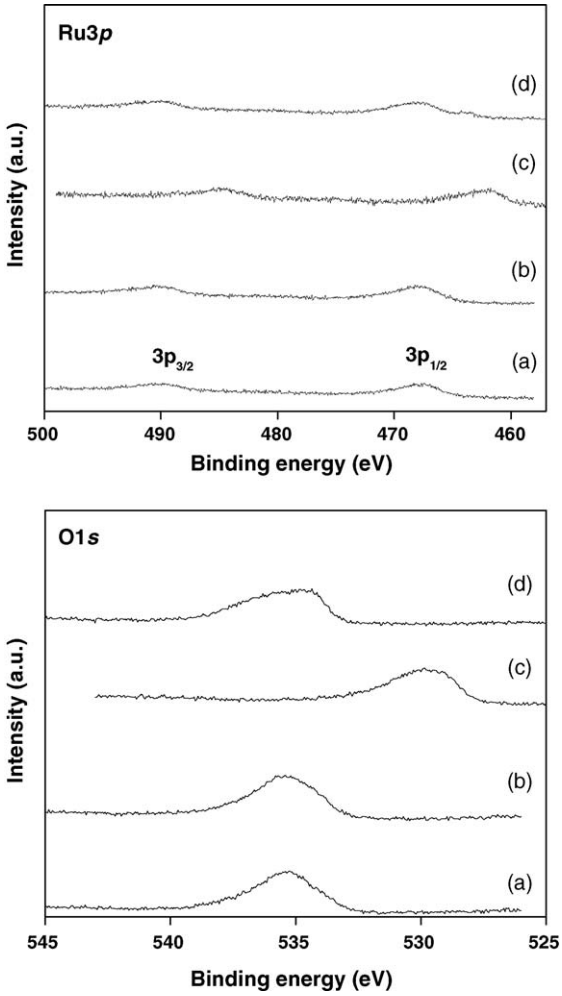

Fig. 4. XPS spectra of $RuO_2{\cdot}xH_2O$ either (a) as-prepared, or annealed in air for 2 h at (b) 100 °C, (c) 200 °C, and (d) 400 °C.

of electrodes fabricated by various physical and/or chemical processes.

Typical specific capacitance versus voltage plots of $RuO_2{\cdot}xH_2O$ electrodes annealed at various temperatures are shown in Fig. 5. Here, the specific capacitance is defined as the ratio of the average capacitance to the geometry area, while the average capacitance was obtained by integrating the cyclic voltammetry response from 0.1 to 0.9 V. As depicted in Fig. 5, the response of pristine $RuO_2{\cdot}xH_2O$ is not stable but improved by annealing at 100 °C. After 200 °C annealing treatment, the capacitive behavior of the oxide is further enhanced as evidenced by the square-like shape of the plot, which according to Conway [1] is a result of a nearly ideal capacitor. Nevertheless, a significant decrease in specific capacitance is observed when the annealing temperature is raised to 400 °C.

The above results demonstrate that the capacitive performance of $RuO_2{\cdot}xH_2O$ electrodes is optimized at an annealing temperature of 200 °C. At this critical temperature, T_{cr}, the electron and proton transports are balanced and there is a high access of both electrons and protons throughout the structure. A schematic mechanism of the carrier transport in the oxide is presented in the capacitance vs. annealing temperature plot,

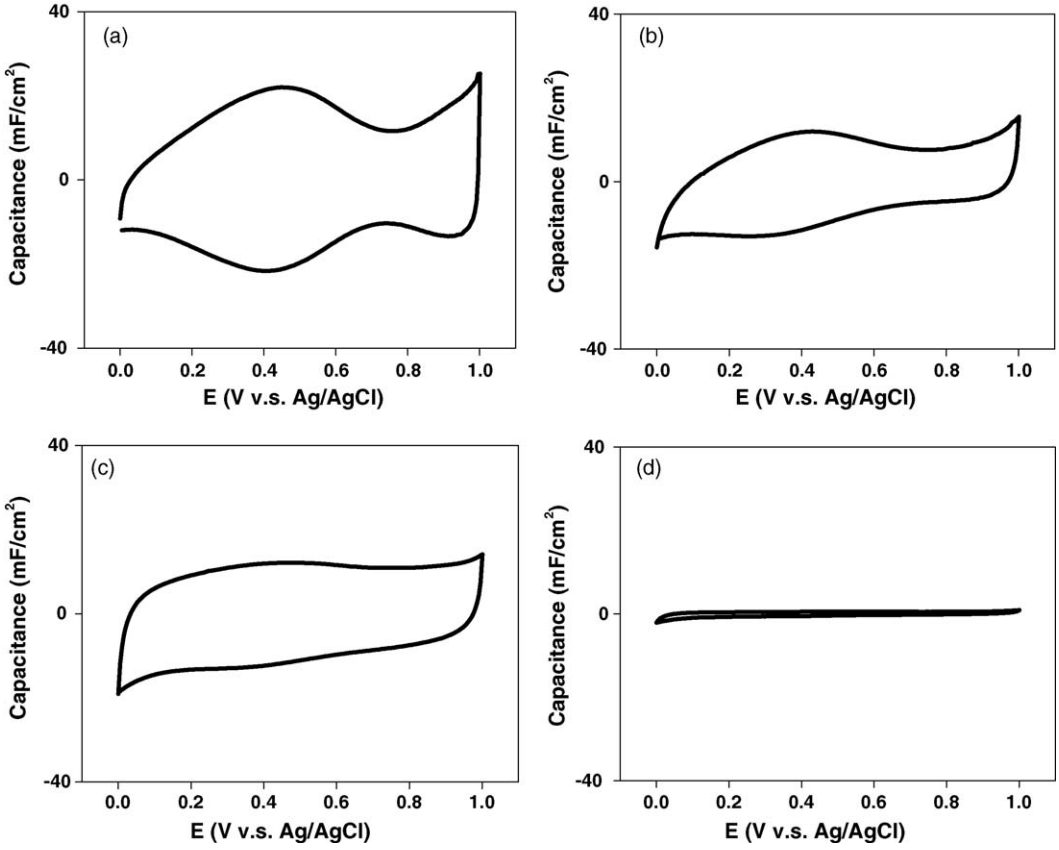

Fig. 5. Cyclic voltammograms (CVs) of $RuO_2 \cdot xH_2O$ either (a) as-prepared, or annealed in air for 2 h at (b) 100 °C, (c) 200 °C, and (d) 400 °C.

Fig. 6. It is well known that anhydrous RuO_2 is composed of RuO_6 octahedra [11,12]. Below the critical annealing temperature, hydrous RuO_2 exhibits a short-range disordering of RuO_6 octahedra. Once the annealing temperature exceeds the critical point, the structure converts to an ordered one with either short- or long-range ordering. The molecular water component of the oxide is decreased and insufficient water cannot efficiently transfer protons to contribute to the capacitive reaction, thereby giving rise to a poor capacitive response. On the contrary, this situation favors the electron conductivity, which is enhanced by the rutile structure of RuO_2. At low annealing temperatures (<200 °C), proton conductivity is promoted because of sufficient hydrogen ions available in the oxide, whereas electronic conductivity is suppressed due to isolation of the RuO_2 by the hydrous matrix. Only at the critical temperature, there is adequate connectivity on the ruthenium oxide and hydrous matrix that can provide long-range electron and proton conduction, respectively [13].

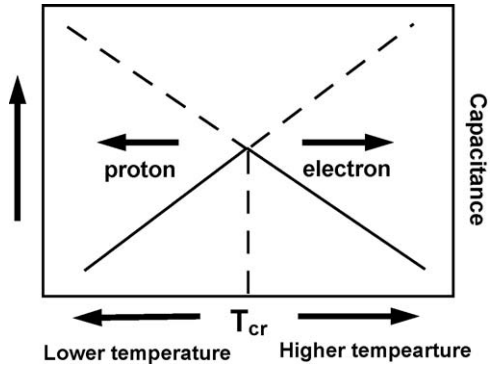

Fig. 6. Schematic illustration of the mechanism of carrier transports in hydrous ruthenium oxides in a capacitance vs. annealing temperature plot.

4. Conclusion

In summary, the effect of annealing temperature on the structure and electrochemical behavior of $RuO_2 \cdot xH_2O$ electroplated on Ti substrate has been investigated. By annealing the sample at 200 °C, which is the threshold temperature for crystallization of ruthenium oxide, the capacitive response was optimized. XRD, XPS and Raman spectra revealed the occurrence of phase transformations at the critical temperature. The high capacitance observed at 200 °C implies that the nanostructure in the oxide supports the establishment of interpenetrating percolation paths for balanced electronic and proton conduction. This study provides a solution to the essential issue of how to obtain an electrode with enhanced electrochemical performance for application in microsupercapacitor.

Acknowledgement

This work was supported by the National Science Council and Ministry of Education in Taiwan.

References

[1] B.E. Conway, Electrochemical Supercapacitors—Scientific Fundamentals and Technological Applications, Kluwer Academic Publishers/Plenum Press, New York, 1999.
[2] K. Shokoohi, J.M. Tarascon, B.J. Wilkens, Appl. Phys. Lett. 59 (1991) 1260.
[3] B.J. Neudecker, N.J. Dudney, J.B. Bates, J. Electrochem. Soc. 147 (2001) 517.
[4] J.H. Park, J.M. Ko, O.O. Parka, J. Electrochem. Soc. 150 (2003) A864.
[5] J.P. Zheng, Electrochem. Solid-State Lett. 2 (1999) 359.
[6] J.R. Zhang, D.C. Jiang, B. Chen, J.J. Zhu, L.P. Jiang, H.Q. Fang, J. Electrochem. Soc. 148 (2001) A1362.
[7] B.E. Conway, V. Birss, J. Wojtowicz, J. Power Sources 66 (1997) 1.
[8] S.Y. Mar, C.S. Chen, Y.S. Huang, K.K. Tiong, Appl. Surf. Sci. 90 (1995) 497.
[9] Y.B. Mo, W.B. Cai, J. Dong, P.R. Carey, D.A. Schersona, Electrochem. Solid-State Lett. 4 (2001) E37.
[10] K.H. Chang, C.C. Hu, J. Electrochem. Soc. 151 (2004) A958.
[11] S. Trasatti, G. Lodi, Electrodes of Conductive Metallic Oxides, Elsevier, Amsterdam, 1981 [Part B, Chapter 10].
[12] P.H. Triggs, Phys. Acta 58 (1985) 657.
[13] R.A. Huggins, Ionics 3 (1997) 379.